Available online at www.sciencedirect.com
ScienceDirect
Scripta Materialia 65 (2011) 569–572
Scripta MATERIALIA
www.elsevier.com/locate/scriptamat

# Finite-element analysis of dimensional non-isotropy during phase transformation in microstructurally banded steel

Yi-Gil Cho,[a] Dong-Woo Suh,[b] Jae Kon Lee[c] and Heung Nam Han[a,*]

[a]*Department of Materials Science and Engineering and Center for Iron & Steel Research, RIAM, Seoul National University, Seoul 151-744, Republic of Korea*
[b]*Graduate Institute of Ferrous Technology, Pohang University of Science and Technology, Pohang 790-784, Republic of Korea*
[c]*Sheet Products and Process Research Group, Technical Research Laboratories, POSCO, Pohang 790-785, Republic of Korea*

Received 25 April 2011; revised 7 June 2011; accepted 7 June 2011
Available online 14 June 2011

Steels with microstructural bands show dissimilar dilatometric behavior depending on the direction monitored. This behavior was simulated using finite-element analysis combining thermal, elasticity, conventional plasticity and transformation plasticity. The results suggest that transformation plasticity plays a major role in generating the characteristic dilatometric behavior derived from dimensional non-isotropy during transformation.


*Keywords:* Superplasticity; Phase transformations; Finite element analysis; Steels; Non-isotropy

Microstructural bands in steels are alternating layers of ferrite and pearlite. They originate from the alignment of segregated regions with substitutional elements during casting and subsequent hot-rolling, which eventually produces layers with different microstructural constituents [1]. A number of studies [2–5] have considered the correlation between the microstructural directionality and dimensional non-isotropy, which is associated with non-isotropic volume changes during a phase transformation. Jaramillo et al. [3,4] described the dimensional non-isotropy in an artificially banded steel using experimental and numerical analyses. Distinct dilatometric behaviors have been reported with respect to the specimen orientation, and a two-cell simulator was used to interpret the results considering the transformation plasticity model proposed by Prantil et al. [6]. Although Jaramillo et al.'s two-cell model captured the dependence of the dimensional non-isotropy on the orientations of the banding pattern, it is difficult to apply this model to a real microstructure because of its simplicity. Furthermore, their model could not consider the dimensional non-isotropy that was also observed in the microstructurally homogeneous specimen, which is reproduced in rigorous modeling. Suh et al. [5] reported the dilatometric analysis of a phase transformation and considered the non-isotropic effect due to microstructural banding. The analysis was in good agreement with the experimentally measured transformation kinetics, but the origin of dimensional non-isotropy was not given in a quantitative manner.

Recently, a numerical model that could simulate the dimensional non-isoptropy in dilatometry was proposed [7]. The model with transformation plasticity was incorporated into a finite-element analysis, and the dimensional non-isotropy during a transformation was interpreted successfully for steels with a homogeneous microstructure. In this study, the orientation-dependent dilatometric behavior in microstructurally banded steel was simulated using finite-element analysis combining thermal, elasticity, conventional plasticity as well as transformation plasticity.

Low-carbon steel (0.14C–1.1Mn–0.11Si, in wt.%) was hot rolled from a 220 mm thick slab to a plate 20 mm thick at temperatures ranging from 1200 to 950 °C. Figure 1a shows the microstructure of the hot-rolled plate. Microstructural bands parallel to the rolling direction can be clearly seen. Cylindrical dilatometric specimens 3 mm in diameter and 10 mm long were machined for two orientations: (i) the longitudinal direction parallel to the banded layer (RD specimen); and (ii) perpendicular to the banded layer (ND specimen). A quench dilatometer was used to monitor the change in length of the specimen during heat treatment. The specimens were heated to 950 °C at a rate of 1 °C $s^{-1}$, held at

* Corresponding author. Tel.: +82 2 880 9240; fax: +82 2 885 1748; e-mail: hnhan@snu.ac.kr

1359-6462/$ - see front matter © 2011 Acta Materialia Inc. Published by Elsevier Ltd. All rights reserved.
doi:10.1016/j.scriptamat.2011.06.012

that temperature for 1 min, then cooled to ambient temperature at a rate of 0.3 °C $s^{-1}$.

Transformation plasticity describes the deformation with stress below the yield strength of a material, which is observed during phase transformation. From a microstructural point of view, two descriptions of transformation plasticity are generally accepted. One is the Magee [9] model, which is based on the formation of variant selection due to the applied stress in a displacive transformation. The other is the Greenwood–Johnson [10] model, which is based on the microplastic strain developing in the weaker phase due to volume mismatch between two phases. Although most existing models for transformation plasticity in a reconstructive transformation are based on the Greenwood–Johnson model, Han et al. [8,11,12] suggested that the Greenwood–Johnson model might not properly explain the transformation during plastic deformation observed experimentally. They suggested a model based on migrating interface diffusion [8] formulated as accelerated Coble creep. This model successfully captured the dimensional non-isotropy occurring in dilatometry [7], and was employed in the present study to describe the transformation plasticity in microstructually banded steels.

A constitutive equation representing the transformation plastic strain increment is described as a function of the transformation increment at a given time step, temperature and applied stress as follows:

$$d\varepsilon^{TP} = \frac{1}{3}\frac{d_0}{\delta} dX \frac{\sigma\Omega}{k_B T} c_{v0} \exp\left(-\frac{Q_f}{k_B T}\right), \quad (1)$$

where $d_0$, $\delta$, and $\Omega$ are the initial grain size of the parent phase, the effective thickness of the interface and the volume of the vacancy, respectively. The Boltzmann constant, $k_B$, has a value of $1.38 \times 10^{-23}$ J $K^{-1}$. $c_{v0}$ is a dimensionless constant determined by the change in thermal entropy associated with the formation of a vacancy, $Q_f$ is the formation enthalpy of a vacancy at the interface, $\sigma$ is the applied stress, and $dX$ is the transformation increment. The initial grain size for the austenite phase of the steel was assumed to be 30 μm. The parameters of Ω, $\delta$ and $Q_f$ were $1.21 \times 10^{-29}$ $m^3$ [13], 1 nm and 80 kJ $mol^{-1}$ [8,12], respectively. The only unknown parameter, $c_{v0}$, was obtained using the constrained Rosenbrock technique [14], which minimized the sum of the squared differences between the experimental and calculated data. The best-fitting value of 0.036 was applied for subsequent calculations.

For the finite-element model, the Cauchy stress increment, $d\sigma$, is represented as follows:

$$d\sigma = C^e : d\varepsilon^e, \quad (2)$$

where $C^e$ and $d\varepsilon^e$ are the elastic stiffness tensor and elastic strain increment, respectively. The total strain rate, $d\varepsilon^T$, is decomposed into four components as follows:

$$d\varepsilon^T = d\varepsilon^e + d\varepsilon^p + d\varepsilon^v + d\varepsilon^{TP}, \quad (3)$$

where $d\varepsilon^p$ is the conventional plastic strain increment, and $d\varepsilon^v$ is the volumetric strain increment due to a phase transformation and temperature variation. $d\varepsilon^{TP}$ represents the transformation plastic strain increment described in Eq. (1).

Tables 1 and 2 list the thermal [15], elastic [16,17] and plastic [18] properties. The densities of austenite and ferrite were defined as functions of the temperature and chemical composition by Miettinen's data [19]. For the density of the pearlite phase, the linear mixture rule was assumed according to the eutectoid composition of the steel. Other thermal properties, such as the heat capacities and heat of transformation were calculated using Thermo-Calc [20]. The constitutive models were incorporated into the user material subroutine, UMAT, of ABAQUS/Standard [21], a commercial software used for implicit finite-element analysis.

A finite-element mesh was designed, as shown in Figure 1b and c. Only 1/8 of the specimen geometry was considered due to the symmetry of the dilatometric specimen. Given the final microstructure and measured phase fractions, the specimens are supposed to transform from austenite to ferrite in the blue layer initially, and then transform to pearlite upon cooling. The transformation kinetics of ferrite and pearlite in each layer were assumed to follow the kinetics obtained by the lever rule from the experimentally measured strains in Figure 2. In the finite-element calculation, the following three assumptions were made:

(1) Uniform temperature profiles at the curved surface of the cylindrical specimen during cooling.
(2) Uniform pressure (0.19 MPa) on the planar surface of the cylindrical specimen due to hard contact between the holder and specimen.
(3) The interfaces between the layers are maintained without sliding, debonding or cracking.

To examine the effect of transformation plasticity on the non-isotropic dilatations, numerical calculations were carried out in two different ways: not considering transformation plasticity, and hence only taking into account the elastic, conventional plastic and volumetric deformations (Fig. 2a); and considering the transformation plasticity as well (Fig. 2b). Figure 2 compares the

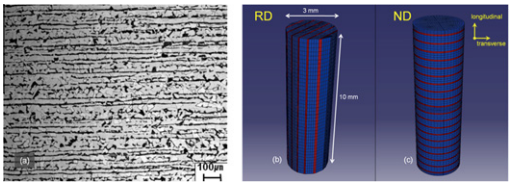


**Figure 1.** (a) Microstructure of the hot-rolled steel. (b and c) Finite-element mesh for the dilatometric specimens: (b) RD specimen showing the longitudinal direction parallel to the rolling direction, and (c) ND specimen showing the longitudinal direction perpendicular to the rolling direction.

**Table 1.** Thermal [15] and elastic [16,17] properties of the steel.

| Temperature, °C | −56 | 25 | 300 | 600 | 700 | 800 |
|---|---|---|---|---|---|---|
| *A* | | | | | | |
| E | 183 | 179 | | | | 140.7 |
| ν | 0.22 | 0.26 | | | | 0.31 |
| *F*, *P* | | | | | | |
| E | | 210.3 | 163 | 144 | 131 | |
| ν | | 0.28 | 0.28 | 0.31 | 0.31 | |
| k | | 36 | 35 | 31 | 31 | |

A, austenite; F, ferrite; P, pearlite; E, Young's modulus (GPa); ν, Poisson's ratio; k, thermal conductivity (W $m^{-1}$ °$C^{-1}$).